Scanning Kelvin Probe Microscopy investigation of optically induced charge in Au nanoparticles embedded into ZrO_2(Y) films

© *D.O. Filatov,*[1] *A.S. Novikov,*[1] *M.E. Shenina,*[1] *I.N. Antonov,*[2] *A.V. Nezhdanov,*[3]
I.A. Kazantseva,[3] *O.N. Gorshkov*[1]

[1] Research and Education Center for Physics of Solid State Nanostructures, Lobachevskii University of Nizhnii Novgorod,
603022 Nizhnii Novgorod, Russia
[2] Research Institute for Physics and Technology, Lobachevskii University of Nizhnii Novgorod,
603022 Nizhnii Novgorod, Russia
[3] Department of Physics, Lobachevskii University of Nizhnii Novgorod,
603022 Nizhnii Novgorod, Russia
e-mail: dmitry_filatov@inbox.ru

Accumulation and relaxation of optically induced electric charge in ZrO_2(Y) films with embedded single-layered arrays of Au nanoparticles (NPs) of $2-3$ nm in diameter have been studied subject to the depth of the Au NPs in the ZrO_2(Y) layers and the optical excitation power at the wavelengths of 473 and 633 nm by Scanning Kelvin Probe Microscopy (SKPM).

Keywords: thin film systems, zirconia, nanoparticles, plasmon resonance.

Introduction

Metallic and semiconductor nanoparticles (NPs) in dielectric films are considered future-oriented for the creation of non-volatile computer memory (the so-called nanoflash memory) on their basis [1]. The basic element of this type of memory is an MIS transistor, in the gate dielectric the NP array is built-in, it acts as a floating gate: NPs, which are potential wells (traps) for electrons, capture the electric charge injected into them and keep it for a long time.

Scanning Kelvin probe microscopy (SKPM) is a powerful method for studying the processes of electric charge local accumulation in such nanocomposite systems [2,3]. In [4] a local charging of a ZrO_2(Y) film with Au NPs embedded in its thickness was detected upon photoexcitation at a plasmon resonance (PR) wavelength in Au NPs. The observed phenomenon was related to the internal photoemission of electrons from Au NPs in ZrO_2(Y). Using this effect, it is possible to create various new optoelectronic devices, for example, image detectors with memory, etc. Besides, charging of NPs due to the electrons photoemission from them was associated with the previously discovered enhancement of the resistive switching (RS) effect in similar nanocomposite films upon photoexcitation at a wavelength of PR [5,6]: NP charging leads to a local increasing of the electric field strength near the NP surface, which, in turn, stimulates the growth of conducting filaments between the electrodes of the memristor structure.

In the present paper the photoinduced charge relaxation processes in ZrO_2(Y) films with Au NPs arrays embedded at different distances from the conducting substrate are studied by the SCPM method.

1. Experimental part

The structure of the samples under examination is shown in Fig. 1. ZrO_2(Y) (12 mol.% Y_2O_3) films 10 nm thick with single layer Au NPs arrays were formed on glass substrates with transparent conducting sublayer of a mixture of In-Sn (indium-tin oxide, ITO) oxides 40 nm thick by layer-by-layer magnetron deposition of ZrO_2(Y)/Au/ZrO_2(Y) sandwich structures using a Torr International MSS-3GS vacuum unit for thin film deposition. ZrO_2(Y) layers were deposited at the substrate temperature $T_g = 300°C$ by high-frequency magnetron sputtering, Au layers — at $T_g = 200°C$ by DC magnetron sputtering. After deposition the sandwich structures were annealed in air at 450°C for 2 min. A more detailed procedure for the formation of ZrO_2(Y) films with Au NP arrays, as well as the results of studies of their structure and optical properties are given in [7,8]. According to the data of high-resolution transmission electron microscopy on transverse sections the Au island film ~ 1 nm thick ruptures upon annealing under the indicated conditions and coagulates into NPs with a diameter of $D = 2-3$ nm, located practically in one plane at fixed distances from the film surface and the film substrate interface (which, in turn, are determined by the thicknesses of the coating and underlying oxide layers). The thickness of the ZrO_2(Y) layer between the Au NP array and the surface of the ITO sublayer d was 5, 3 and 0 nm (Fig. 1, $c-e$ respectively); in the latter case the Au film was deposited
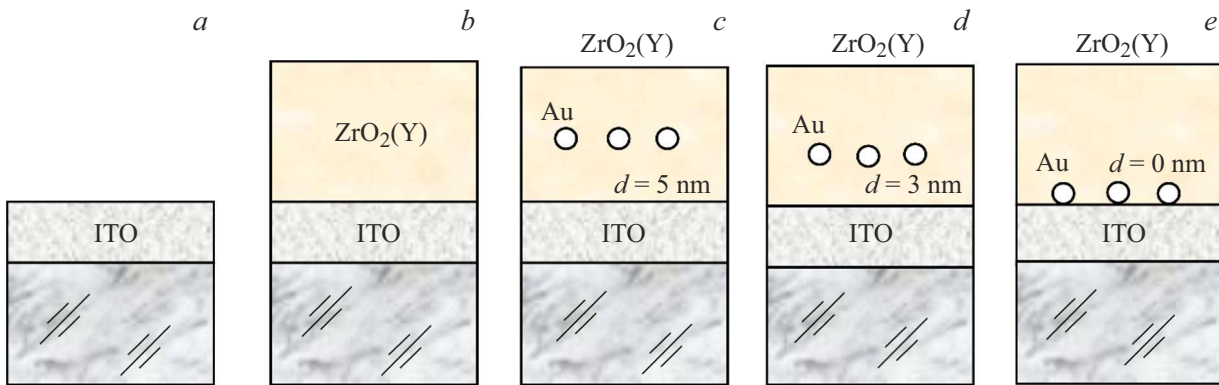
Figure 1. Structure of the studied samples: a, b — samples for comparison with the ITO layer and $ZrO_2(Y)$ film without Au NPs, respectively; $c-e$ — $ZrO_2(Y)$ films with Au NPs located at different distances from the ITO sublayer d, nm: c — 5, d — 3, e — 0 (Au NP array adjoins the surface of the ITO sublayer).

directly onto the ITO surface. As samples for comparison we used $ZrO_2(Y)$ film 10 nm thick without Au NPs formed on glass substrate with an ITO sublayer (Fig. 1, b), as well as a glass substrate with ITO film on the surface (Fig. 1, a).

Investigations by the SKPM method were carried out on a microspectroscopic complex NT-MDT NTegra Spectra at 300 K. NT MDT NSG-11 probes with TiN coating were used. Photoexcitation was carried out from the substrate side by a laser diode at a wavelength $\lambda = 473$ nm and by He−Ne laser with $\lambda = 633$ nm. The radiation was focused onto the surface of $ZrO_2(Y)$:LF-Au film into a spot 1 μm in diameter. The optical properties of the samples studied in this paper were previously studied by optical transmission spectroscopy at 300 K using a Varian Cary 6000i spectrophotometer [4]. It was found that the radiation with $\lambda = 633$ nm corresponds to the PR peak in Au NPs, while the short-wavelength radiation with $\lambda = 473$ nm is outside the PR band. The laser radiation power P varied within 1 μW−3.4 mW. The surface electric potential induced by radiation on the surface of the $ZrO_2(Y)$ film was registered after the laser turning off at regular intervals (15 or 30 min) using the standard two-pass method (probe elevation 10 nm). The ITO conducting layer was grounded.

Note that under the experimental conditions, uncontrolled charging of the sample surface is possible due to the electrons photoemission from the Au NPs under the action of the radiation of the NTegra scanning head alignment laser with a radiation wavelength of 650 nm, which falls on the edge of the PR band in the Au NP array. Other reasons for the appearance of the uncontrolled background potential on the surface of the samples are also possible, for example, the accumulation of a static electric charge, etc. To reveal the effect of local external illumination by laser radiation against the background of the specified uncontrolled background potential, the background was subtracted from the obtained SKPM images. To do this, we used an approximation by a second-order surface, which was carried out through the edges of the SKPM image far from the charge spot.

2. Results and discussion

On SKPM images of the surface of $ZrO_2(Y)$ films with Au NPs in places subjected to laser irradiation at wavelengths $\lambda = 633$ and 473 nm the local changes in the surface electric potential (charge spots, Fig. 2, $a-c$) were observed, they persisted for a relatively long time (up to a day, and in some cases even longer) after the laser was turned off. It was found earlier in [4] that the appearance of charge spots is associated with the Au NPs charging due to internal photoemission of electrons from Au NPs into $ZrO_2(Y)$ (Fig. 3). The height of the potential barrier between the Fermi level in Au NPs E_F and the bottom of the conducting band in $ZrO_2(Y)$ E_c is 2.5 eV [9]. In this connection, under photoexcitation at a wavelength of $\lambda = 473$ nm (corresponding photon energy $hv = 2.6$ eV), photoemission of electrons from the Fermi level in Au NPs can occur into the conducting band of $ZrO_2(Y)$ (process $1b$ in Fig. 3, a).

At $\lambda = 633$ nm, the quantum energy $hv = 1.96$ eV is not enough to eject the electron from the Fermi level of Au NPs into the $ZrO_2(Y)$ conducting band, but it is sufficient to eject the electron into the vacancy α-band in $ZrO_2(Y)$ (process $1a$ in Fig. 3, a).

On reference samples $ZrO_2(Y)$/ITO (Fig. 1, b) and ITO layer (Fig. 1, a) the residual charge spots were also observed on glass substrates after exposure to laser radiation (Fig. 2, d). In this case, the charge spots can be associated with the photoionization of deep levels in the $ZrO_2(Y)$ film and/or in the glass substrate [4]. In the latter case, local accumulation of long-lived photoinduced positive charge is possible only in a thin (thickness about the diffusion length of electrons in glass) subsurface layer of the substrate near its interface with the ITO layer. Only in this case, the photoexcited electrons have the opportunity to escape into the ITO layer before they are captured back on the photoionized traps. On the contrary, during photoionization of traps deep in the substrate, the capture of photoexcited electrons back on the traps is more probable. Such process
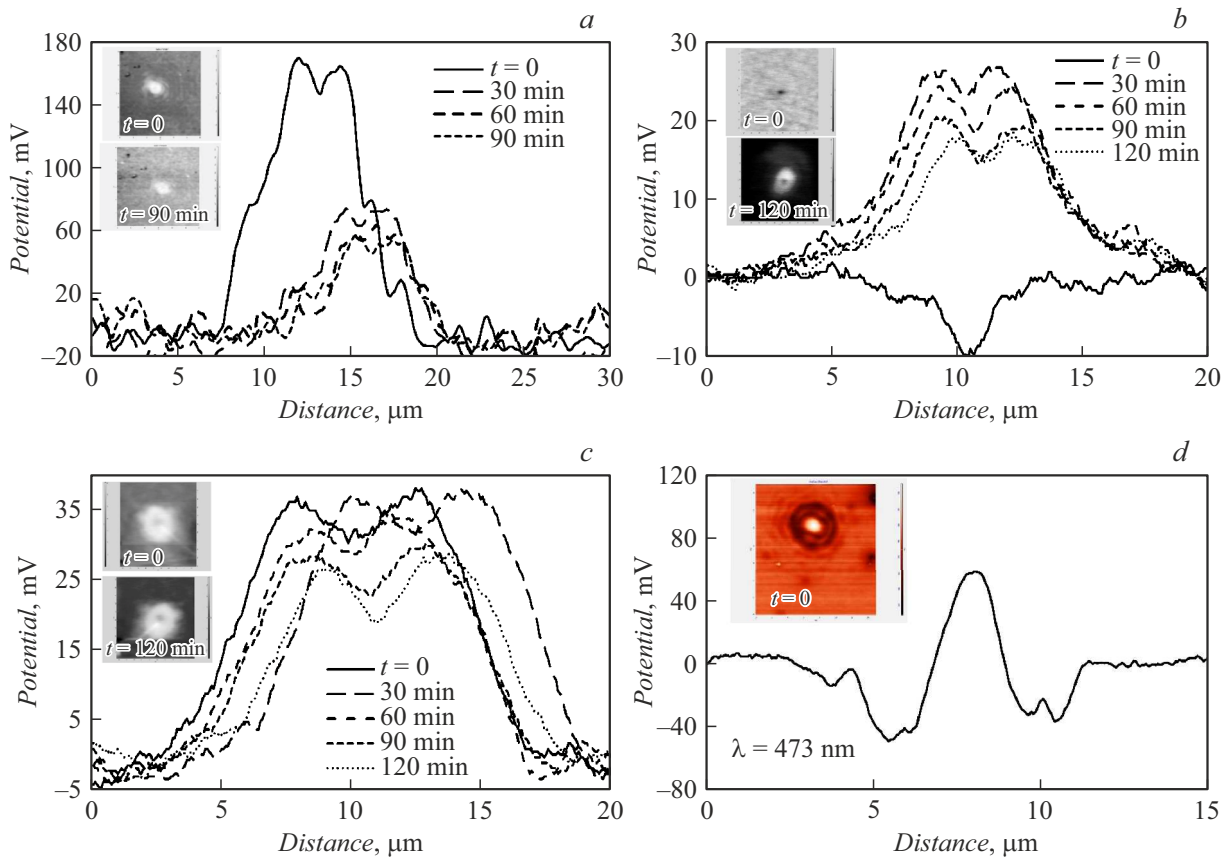
Figure 2. Potential profiles of charge spots after surface irradiation of $ZrO_2(Y)$:LF-Au: a — $d = 5$ nm, $\lambda = 473$ nm, $P = 6\,\mu$W; b — $d = 0$ nm, $\lambda = 633$ nm, $P = 2.5$ mW; c — $d = 0$ nm, $\lambda = 473$ nm, $P = 3.4$ mW. d — reference sample $ZrO_2(Y)$/ITO: $t = 0$, $\lambda = 473$ nm, $P = 3.4$ mW. In inserts: SCPM images of the charge spot at the initial and final moments of time after the laser is turned off.

does not violate the overall electrical neutrality of the sample and cannot lead to the accumulation of a long-lived positive charge near its surface.

Photoionization of these deep levels apparently also takes place in films with Au NPs. To separate the contributions of photoionization of Au NPs and deep levels to the formation of charge spots on the surface of $ZrO_2(Y)$:NP-Au films, the kinetics of charge spot relaxation was studied. Fig. 4 shows the dependences of the values of the maximum potential φ_m of the profiles drawn through the centers of charge spots (Fig. 2) on the time t elapsed since the laser was turned off, this is for various samples and wavelengths of photoexcitation. A higher value φ_m at the initial time moment t (by up to 3 times exceeding the steady state value) was observed for $ZrO_2(Y)$:NP-Au samples with $d = 5$ nm at $\lambda = 473$ nm (Fig. 4, a and process $1b$ in Fig. 3, a), when the thickness of the tunneling barrier for electrons is maximum, and the photoemission of electrons occurs into the conducting band of $ZrO_2(Y)$. As the time elapsed since the laser was turned off t (both during photoexcitation with $\lambda = 473$ nm and with $\lambda = 633$ nm (Fig. 4)) the charge spot potential decreased. This is due to the neutralization of the positive charge that appears on Au NPs due to photoemission of electrons

during photoexcitation, due to electrons flowing into NPs from the ITO layer by tunneling [4] (process 2 in Fig. 3, a).

The characteristic time of electron tunneling from the ITO layer into Au NPs can be estimated as follows. The tunneling transparency T of the $ZrO_2(Y)$ potential barrier between Au NPs and the ITO sublayer can be estimated using the well-known semiclassical formula for the tunneling transparency of a trapezoidal potential barrier

$$T \sim \exp\left(-\frac{2l}{\hbar}\sqrt{2mU}\right), \qquad (1)$$

where U — average height of potential barrier, m — effective electron mass in $ZrO_2(Y)$, $\hbar$ — Planck's constant, l is the width of the potential barrier (the thickness of the $ZrO_2(Y)$ layer between the Au NP surface and the interface with the ITO sublayer). Under equilibrium conditions, the rate of electron tunneling from ITO to Au NPs is equal to the rate of the reverse process. For the electron at the Fermi level in the Au NP $U = (E_{Au} + E_{ITO})/2$, where $E_{ITO} = E_{c1} - E_F$, $E_{Au} = E_{c2} - E_F$, E_{c1} and E_{c2} are energy values of the bottom of the valence band in $ZrO_2(Y)$ at the boundaries ITO/$ZrO_2(Y)$ and $ZrO_2(Y)$/Au respectively (Fig. 4, a). Assuming for Au NP in $ZrO_2(Y)$ $E_{Au} = 2.5$ eV [9], $E_{ITO} = X_{YSZ} - A_{ITO} = 2.2$ eV
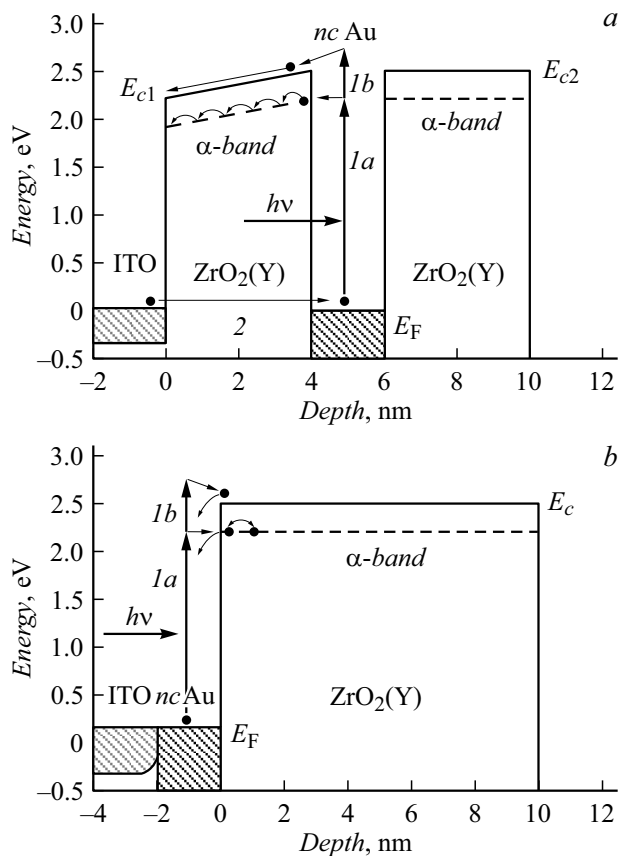
Figure 3. Calculated energy band diagrams (300 K) and diagrams of electrons photoexcitation and photoinduced charge relaxation for $ZrO_2(Y):NP-Au/ITO$ structures with NP depth d, nm: a — 5, b — 0.

($X_{YSZ} = 2.3$ eV [10] and $A_{ITO} = 4.5$ eV [11] are values of the electron affinity energy for $ZrO_2(Y)$ and the electron work function for ITO respectively) and $m = 0.4m_0$ [12] (m_0 is free electron mass), we obtain for $l = dD/2 = 4$ nm $T = 5.7 \cdot 10^{-18}$.

The characteristic tunneling time of the electron from Au NP with Fermi energy E_F to the ITO layer can be estimated as $\tau \sim 2D/v_F T$, where v_F is electron velocity at the Fermi level in Au. For $v_F = 1.4 \cdot 10^8$ cm/s [13] we get $\tau \sim 500$ s ~ 8 min, which agrees by magnitude with the characteristic decay time of the potential φ_m in Fig. 4 for $d = 5$ nm. For $d = 3$ nm we get $\tau \sim 10^{-6}$ s, which is much smaller than the characteristic scale of observation time in the experiment. In turn, this allows us to conclude that the decay of the potential φ_m for $d = 3$ nm in Fig. 4 (which depends weakly on time within $t < 120$ min) is determined by the slowly relaxing photoinduced charge of deep levels in $ZrO_2(Y)$ layer and/or in the glass substrate, the relaxation time of which considerably exceeds the relaxation time of charge in NP [4].

Note that φ_m values for the $ZrO_2(Y)/ITO$ reference sample were significantly smaller than for the sample representing ITO layer on glass substrate, both for $\lambda = 473$ nm

(Fig. 4, a) and for $\lambda = 633$ nm (Fig. 4, b). This indicates that the charge spots observed on the reference samples are due to the photoinduced charge of deep levels localized in the glass substrate near its interface with the ITO layer.

In the case of photoionization of deep levels localized in ITO, due to the significant concentration of conducting electrons in ITO layers in the studied samples ($\sim 10^{21}$ cm^{-3} according to Hall measurements), also we can expect a rapid neutralization of the photoionized deep levels, which excludes the possibility of observing the residual charge associated with these levels.

Note also that the steady state value φ_m for $d = 5$ nm in Fig. 4, a at $P = 33\,\mu$W was significantly higher, than for $P = 6$ and $1\,\mu$W. This shows that the photoinduced charge density of deep levels in the substrate increases with the radiation power increasing. At the same time, the initial values of φ_m are practically the same for $P = 6$ and $33\,\mu$W. As was established in [4], that the average charge of NPs under experimental conditions similar to those of the experiments performed in this paper is elementary charge ~ 1. Due to the low capacitance of the NP relative to the ITO electrode, the emission of even one electron from the NP leads to significant change in its potential relative
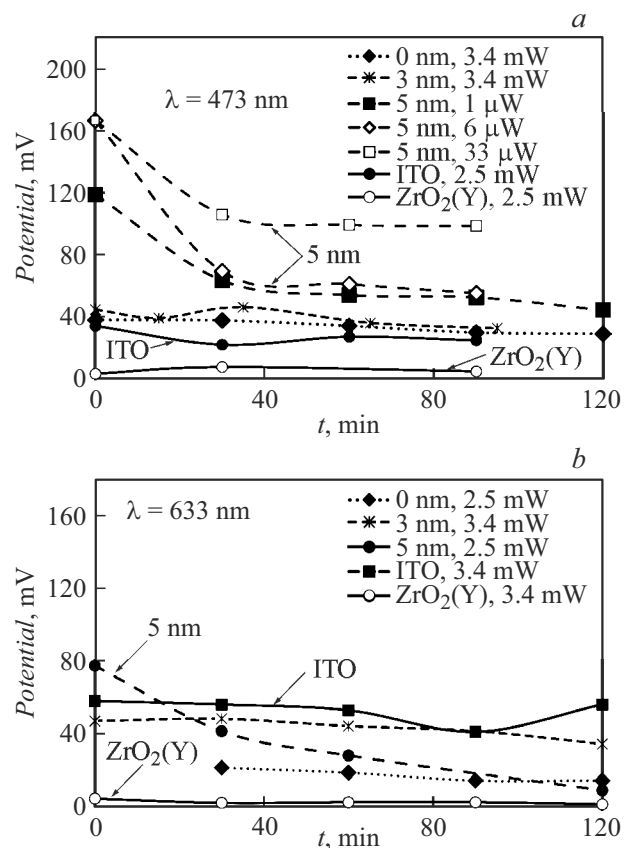
Figure 4. Maximum charge spot potential φ_m, measured at regular time intervals t, for $ZrO_2(Y):NP-Au/ITO$ structures (Fig. 1, $c-e$), as well as for reference samples $ZrO_2(Y)/ITO$ and the ITO layer (Fig. 1, a, b), from the moment the photoexcitation is turned off with the laser wavelength λ, nm: a — 473, b — 633.

to the ITO sublayer (by ~ 0.1 V), which leads to significant height increasing of the potential barrier between Au NPs and ITO layer. In turn, this limits the photoemission of the second electron from the Au NPs.

In the sample with a depth of Au NPs occurrence $d = 0$ nm, during photoexcitation at wavelength of $\lambda = 633$ nm, immediately after the laser turning off ($t = 0$), a spot of local negative charge was observed (Fig. 2, b). In the course of relaxation, the potential of the irradiated region first rapidly increases and becomes positive, and then decreases relatively slowly. We attribute this to the competition of two processes:

1) photoexcitation of electrons from Au NPs to α band in the ZrO$_2$(Y) layer, followed by electrons flow into the ITO layer (process *1a* in Fig. 3, b);

2) photoionization of traps in the glass substrate, followed by their neutralization by electrons coming from the ITO layer.

The first process prevails during local illumination by external laser radiation, since the cross section for the photon interaction with the electron at the Fermi level in Au NPs under PR conditions is larger than with the electron captured to deep level. In this case, the positive charge of photoionized Au NPs is quickly neutralized by electrons flowing from the ITO layer. In this connection, immediately after illumination by the laser the induced negative charge is observed in the α band (Fig. 2, b). On the other hand, the negative charge photoinjected into localized states into the α band in the ZrO$_2$(Y) layer flows back into Au NPs and into the ITO layer much faster than the neutralization of the positive charge of photoionized traps in a glass substrate. Therefore, shortly after illumination by external laser radiation the total spot charge is now determined by the positive charge of the photoionized deep levels in the substrate, and the SKPM profiles become positive (Fig. 2, b), although they also exhibit local potential decreasing in the center of spots. A similar feature is also observed in the potential profiles measured on other samples (cf. Fig. 2, a). Note also that no negative potential was observed in the sample with $d = 0$ nm under photoexcitation with $\lambda = 473$ nm (Fig. 2, c). In this case, photoexcitation of electrons from Au NPs into the conducting band in ZrO$_2$(Y) is most likely (process *1b* in Fig. 3, b), from which the electrons are able to flow rather quickly into the Au NPs or into the ITO layer.

Conclusion

In this paper, the accumulation and relaxation of the optically induced electric charge in ZrO$_2$(Y) films with built-in single-layer Au NPs array with a diameter of $2-3$ nm, depending on the depth of Au NPs occurrence in the layer ZrO$_2$(Y) were studied using SCPM method. It was established that relaxation of the photoinduced charge in Au NPs occurs via the electrons tunneling from the conducting ITO sublayer deposited on the glass substrate into Au NPs.

It was also established that the charge spots observed on the surface of the reference samples (ZrO$_2$(Y)/ITO layer and the ITO layer on the surface of the glass substrate) are due to the photoionization of deep levels in the glass substrate localized near its interface with the ITO sublayer. Besides, the effect of negative charge accumulation in the photoexcitation region associated with the photoinjection of electrons from Au NPs under PR conditions into localized electronic states in the vacancy α-band in ZrO$_2$(Y) films was discovered. This effect is most pronounced in the sample where Au NPs are embedded at the interface between the ITO and ZrO$_2$(Y) layers.

Conflict of interest

The authors declare that they have no conflict of interest.

References

[1] T. Chen, Y. Liu. *Semiconductor Nanocrystals and Metal Nanoparticles: Physical Properties and Device Applications* (Boca Raton: CRC Press, 2016)

[2] M.S. Dunaevskiy, P.A. Alekseev, A.N. Titkov, E. Landeranta, A. Lashkul, P. Girard. J. Appl. Phys., **110**, 084304 (2011). DOI: 10.1063/1.3651396

[3] M.N. Koryazhkina, D.O. Filatov, I.A. Antonov, M.A. Ryabova, M.S. Dunaevskii. Poverkhnost: rentgenovskie, sinkhrotron-nye i neytronnye issledovaniya **1**, 45 (2019) (in Russian). DOI: 10.1134/S0207352819010104

[4] A.S. Novikov, D.O. Filatov, M.E. Shenina, I.N. Antonov, D.A. Antonov, A.V. Nezhdanov, V.A. Vorontsov, D.A. Pavlov, O.N. Gorshkov. J. Phys. D: Appl. Phys., **54** (48), 485303 (2021). DOI: 10.1088/1361-6463/ac1d11

[5] A.S. Novikov, D.O. Filatov, D.A. Antonov, I.N. Antonov, M.E. Shenina, O.N. Gorshkov. J. Phys.: Conf. Ser., **993**, 012026 (2018). DOI: 10.1088/1742-6596/993/1/012026

[6] A.S. Novikov, D.O. Filatov, D.A. Antonov, I.N. Antonov, M.E. Shenina, O.N. Gorshkov. Poverkhnost: rentgenovskie, sinkhrotronnye i neytronnye issledovaniya **1**, 52 (2019) (in Russian). DOI: 10.1134/S0207352819010177

[7] O.N. Gorshkov, I.N. Antonov, D.O. Filatov, M.E. Shenina, A.P. Kasatkin, D.A. Pavlov, A.I. Bobrov. Pis'ma v ZhTF **1**, 72 (2016) (in Russian).

[8] O. Gorshkov, I. Antonov, D. Filatov, M. Shenina, A. Kasatkin, A. Bobrov, M. Koryazhkina, I. Korotaeva, M. Kudryashov. Adv. Mater. Sci. Engineer., **2017**, ID 1759469 (2017). DOI: 10.1155/2017/1759469

[9] D. Filatov, D. Guseinov, I. Antonov, A. Kasatkin, O. Gorshkov. RSC Adv., **4**, 57537 (2014). DOI: 10.1039/c4ra10236c

[10] G.V. Samsonov (red.). *Physiko-khimicheskie svoystva okislov. Spravochnik* (Metallurgiya, M., 1978) (in Russian)

[11] *Landolt-Börnstein: Zahlenwerte und Funktionen aus Physik, Chemie, Astronomie, Geophysik, Thechnik* (Springer, Berlin, 1960)

[12] H.A. Abbas. *Stabilized Zirconia for Solid Oxide Fuel Cells or Oxygen Sensors: Characterization of Structural and Electrical Properties of Zirconia Doped with Some Oxides* (LAP Lambert Academic, 2012)

[13] H. Kroemer, C. Kittel. *Thermal Physics* (W.H. Freeman Co, 1980)